Equivalent Circuit Models of Voltage-controlled Dual Active Bridge Converters

R. Mallik*, B. Majmunovic†, S. Mukherjee†, S. Dutta*, G.-S. Seo‡, D. Maksimovic†, and B. Johnson*
*Department of Electrical and Computer Engineering, University of Washington, Seattle, WA 98195, USA
Email: rmallik@uw.edu, sdutta@uw.edu, brianbj@uw.edu
† Department of Electrical, Computer, and Energy Engineering, University of Colorado, Boulder, CO 80309, USA
Email: branko.majmunovic@colorado.edu, satyaki.mukherjee@colorado.edu, maksimov@colorado.edu
‡Power Systems Engineering Center, National Renewable Energy Laboratory, Golden, CO 80401, USA
Email: gabsu.seo@nrel.gov

***Abstract*—In this paper, we introduce a new method of modeling voltage-controlled dual active bridge converters as equivalent circuits. What makes the proposed model unique is that the entire closed-loop system (converter *and* control loop) are represented together in one equivalent circuit. Since the full system can be recast as a circuit, this allows for deeper insights on how the closed-loop system performs and for the direct application of circuit analysis techniques. In particular, we reveal how classical control notions can be understood as circuit laws.**

***Index Terms*—circuit analysis, control systems, converter and control model, dual-active-bridge converters**

I. Introduction

Dual active bridge (DAB) converters are widely used in applications where isolation and high voltage conversion ratios are required [1]. DAB use-cases run the gamut from battery chargers for hybrid electric vehicles [2], to photovoltaic systems [3], and medium-voltage grid-connected converters [4]. It is well-known that switch-cycle-averaged converter models are essential for analysis, control design, and reduced computational complexity. Along these lines, we propose a new modeling approach where *both* the averaged DAB converter *and* its closed-loop voltage controller are represented together as a unified circuit equivalent. After recasting the averaged system as a circuit, it is shown that its closed-loop characteristics naturally emerge from Kirchhoff's laws. Not only does this circuit-based framework reveal a link between circuit and control laws, but it also gives deeper intuition on how the closed-loop DAB system operates.

Impedance-based methods have emerged as a popular approach to analyze the small-signal dynamics of converter systems [5]–[7]. With such a framework, stability can be analyzed in terms of the effective output impedance of a given converter [8] where the output port is modeled as either a Norton or Thevenin equivalent. Although this provides a valuable linkage between the circuit concept of impedance with stability, the converter and its various control loops are not explicitly represented as circuits. In other words, impedance-based approaches do not explicitly reveal the circuit equivalent that captures the feedback and feedforward action.

Generally speaking, classical frequency domain and state-space models provide little physical intuition beyond what can be gleaned from Bode and root-locus plots. To bypass these limitations, a new method for modeling voltage-controlled converters as circuits is established. By casting the closed-loop converter system as a circuit, physical intuition is revealed on how the compensator interacts with the output load, feedback and feedforward sensing paths, and reference signal. After defining the equivalent circuit, Kirchhoff's laws are applied to distill it into a canonical circuit which captures key input-output relations. Finally, we show how superposition along with the voltage and current divider equations directly give us the closed-loop system model without any tedious algebra. Curiously, it emerges that the voltage and current divider equations have a direct mapping to the well-known sensitivity and complementary sensitivity functions that are classically used to analyze closed-loop systems in both the controls [9] and power electronics [10] contexts.

The paper is structured as follows: In Section II, we define notation and modeling basics. We derive the equivalent circuit model in Section III. Section IV establishes a one-to-one correspondence between the circuit and classical control frameworks. Finally, concluding statements are in V.

II. Modeling Preliminaries

Consider the DAB circuit in Fig. 1(a) with dc input voltage, v_i, a $1:n$ transformer which links the two bridges, transformer leakage inductance L, and output voltage v. The secondary active bridge delivers dc current i_o into the dc output. The terminals of the output capacitance C, define the converter load terminals. We model the external load as a nominal resistance R_ℓ, and a disturbance current source i_ℓ, which captures all other load uncertainties.

Funding for the work reported in this paper was provided in part by U.S. Department of Energy Office of Energy Efficiency and Renewable Energy Solar Energy Technologies Office grant number DE-EE0008346. This work was authored in part by the National Renewable Energy Laboratory, operated by Alliance for Sustainable Energy, LLC, for the U.S. Department of Energy (DOE) under Contract No. DE-AC36-08GO28308. The views expressed in the article do not necessarily represent the views of the DOE or the U.S. Government.

978-1-7281-1842-0/19/$31.00 ©2019 IEEE

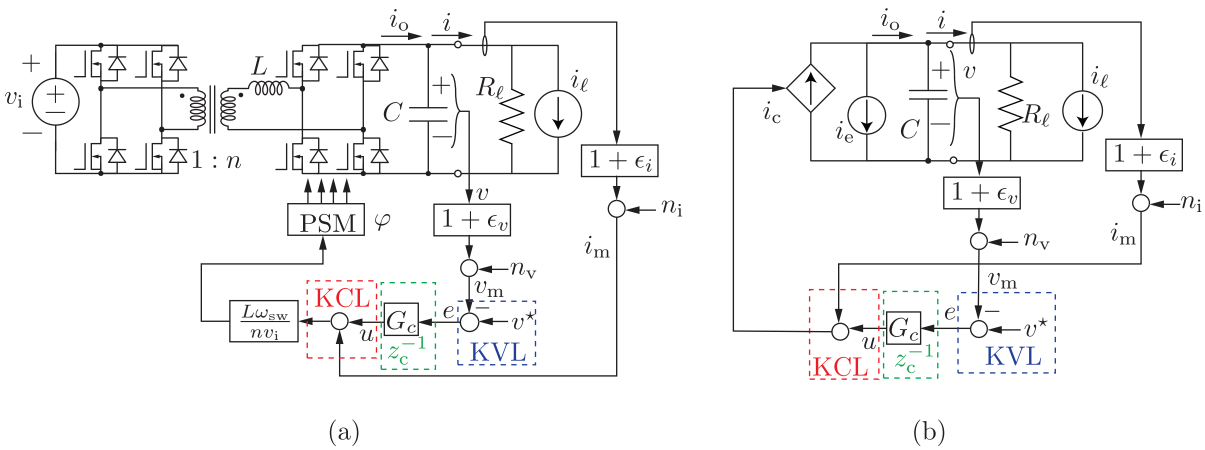

Fig. 1. We analyze a DAB with voltage control. The load is modeled as a nominal resistance in parallel with a current sink. The switched model is in (a) and its switch-cycle-averaged counterpart is in (b).

The feedback loop begins with the sensed load voltage and current. We model the non-ideal voltage and current sensor as having an off-nominal scaling factor ϵ_{v} and ϵ_{i}, respectively, and an additive noise n_{v} and n_{i}, respectively. Hence, the measured load voltage and current, v_{m} and i_{m}, are

$$v_{\mathrm{m}} = (1+\epsilon_{\mathrm{v}})v + n_{\mathrm{v}}, \tag{1}$$
$$i_{\mathrm{m}} = (1+\epsilon_{\mathrm{i}})i + n_{\mathrm{i}}. \tag{2}$$

Reflecting on (1)–(2), ideal sensing is recovered in the limit $\epsilon_{\mathrm{v}}, \epsilon_{\mathrm{i}}, n_{\mathrm{v}}, n_{\mathrm{i}} \to 0$.

The voltage controller acts on the reference $v^\star$ and the compensator, denoted as G_{c}, produces the control effort u. As shown in Fig. 1, the load current i, is added to the control effort as a feedforward signal. The DAB utilizes phase-shift modulation (PSM) where the secondary-side phase shift, denoted as φ, is defined relative to the primary-side switch signal. The switch-cycle-averaged DAB output current is [1]

$$i_{\mathrm{o}} = \frac{v_{\mathrm{i}}\varphi}{nL\omega_{\mathrm{sw}}}\left(1-\frac{\varphi}{\pi}\right) = i_{\mathrm{c}} - i_{\mathrm{e}}, \tag{3}$$

where

$$i_{\mathrm{c}} := \frac{v_{\mathrm{i}}}{nL\omega_{\mathrm{sw}}}\varphi,\; i_{\mathrm{e}} := \frac{v_{\mathrm{i}}}{nL\omega_{\mathrm{sw}}}\frac{\varphi^2}{\pi}. \tag{4}$$

We consider the setting where the the phase shift, φ, is kept small such that $\varphi \gg \varphi^2/\pi$, and hence $i_{\mathrm{c}} \gg i_{\mathrm{e}}$. To simplify implementation and design, we designate the first-order term, i_{c}, as being directly manipulated by the controller. We apply (4) and scale the control output, i_{c}, by $L\omega_{\mathrm{sw}}/nv_{\mathrm{i}}$ to obtain φ (see Fig. 1(a)). Given that the control output is a current signal, we can abstract away the switch modulation and redraw the switched converter in Fig. 1(a) as the circuit in Fig. 1(b) where all variables are averaged over a switch cycle. Averaged quantities are implied throughout from here forward. Note that we retain the second order term, i_{e}, in our averaged model to capture the effect of the small-angle approximation error.

III. Development of the Equivalent Circuit Model

Referring to the averaged model in Fig. 1(b), it is evident that the compensator input-side has a voltage difference whereas the output is a current signal. Accordingly, the compensator can be recast as an admittance that translates the voltage difference $v^\star - v_{\mathrm{m}}$ into a current, u, and the relations on either side of the compensator can be understood via Kirchhoff's laws (see KVL and KCL relations in Fig. 1). This observation allows us to define $z_{\mathrm{c}}^{-1}(s) := G_{\mathrm{c}}(s)$, where $z_{\mathrm{c}}(s)$ is an impedance and its inverse is functionally equivalent to $G_{\mathrm{c}}(s)$. Combining these insights, we redraw the averaged system as the circuit in Fig. 2.

Note that the circuit model in Fig. 2 is an *exact* representation of the averaged model when both are initialized identically. Reflecting on the circuit model, the reference signal $v^\star$, noise n_{v}, and sensor scaling error component $\epsilon_{\mathrm{v}}v$, act as voltage sources and the error voltage, e, is across $z_{\mathrm{c}}(s)$. To summarize, signals on the input-side of the compensator take the form of voltage sources.

Switching focus to the compensator output side, the feedforward current is added to the control effort, u. Since the feedforward and control effort are both current signals, we map the control signals in Fig. 1(b) to a corresponding KCL relationship in Fig. 2. Accordingly, the current sensor noise becomes of a shunt current source and the scaling error effects the controllable current source which models the feedforward. Finally, the modeling error, i_{e}, acts as a current source.

A. The Canonical Circuit Equivalent Model

Once we arrive at the equivalent circuit in Fig. 2, we seek a *canonical* form that clearly emphasizes key input-output relationships. Towards that end, we lump the model non-idealities into composite current and voltage disturbance which we denote as i_{d} and v_{d}, respectively. In particular,

$$i_{\mathrm{d}} = \epsilon_{\mathrm{i}} i_\ell + n_{\mathrm{i}} - i_{\mathrm{e}}, \tag{5}$$
$$v_{\mathrm{d}} = \epsilon_{\mathrm{v}} v + n_{\mathrm{v}}, \tag{6}$$

where i_{d} encapsulates the current sensor scaling error and noise, as well as the small-angle approximation residual. Similarly, v_{d} contains the voltage sensor non-idealities and noise. Due to scaling error in the feedforward current sensor, an exact cancellation of R_ℓ is not possible. After accounting

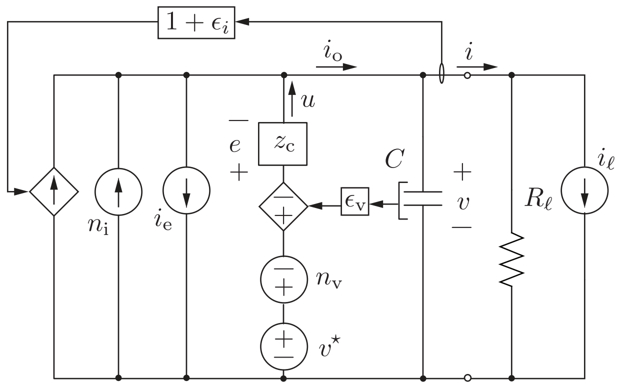

Fig. 2. The equivalent circuit model where the feedback and feedforward control action are translated into equivalent circuit elements. For instance, the setpoint, sensor non-idealities, and modeling errors are interpreted as corresponding voltage and current sources.

for the off-nominal current sensor scaling, the effective load which remains is R_ℓ/ϵ_i. The canonical circuit is in Fig. 3 where we denote the impedance across the output capacitor and uncanceled load as

$$z_p(s) = \frac{1}{sC} \left\| \frac{R_\ell}{\epsilon_i} \right. = \frac{R_\ell/\epsilon_i}{sC + R_\ell/\epsilon_i}. \tag{7}$$

Having arrived at the simplified circuit in Fig. 3 where the disturbances, references voltage, compensator, and load are segregated, we can apply classical circuit analysis methods to compute the closed-loop response. Applying superposition along with the voltage and current divider equations, we obtain

$$\begin{aligned} v(s) = &\frac{z_p(s)}{z_p(s)+z_c(s)} v^\star(s) \\ &- \frac{z_p(s)}{z_p(s)+z_c(s)} v_d(s) + \frac{z_c(s)}{z_p(s)+z_c(s)} z_p(s) i_d(s). \end{aligned} \tag{8}$$

The first and second terms capture how the reference voltage sensor errors are dropped across the series-connected load and compensator impedances. The last term highlights how the current signal nonidealities are divided up between the load and compensator branches.

IV. Translating Circuit Laws into Control Laws

Having computed the closed-loop model in (8) with circuit methods only, we next show how classical control relations can be recovered from our result. This will effectively demonstrate how our circuit-based approach is consistent with classical control frameworks.

A. Closed-loop Models

To draw a clear linkage with established control methods, we will rewrite our model with notation commonly seen in controls analysis. Recall that the compensator transfer function is related to its equivalent impedance by $G_c(s) = z_c^{-1}(s)$. Next, we designate the effective load impedance as being the plant transfer function We define the , where $z_p(s)$ is given in (7). Once we substitute these definitions into (8) and perform

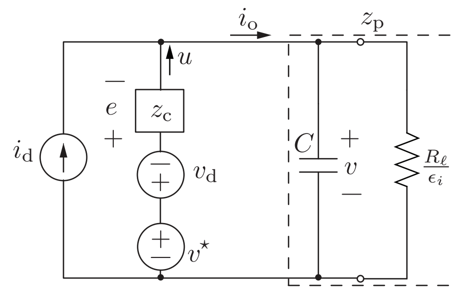

Fig. 3. We obtain the canonical circuit model where all undesirable system characteristics are lumped into one voltage and current source disturbance. This simplified model highlights key input-output relationships and facilitates closed-loop system analysis.

some elementary algebraic manipulations, we recover the well-known relations [9], [10] below:

$$\begin{aligned} v(s) = &\frac{G_p(s)G_c(s)}{1+G_p(s)G_c(s)} v^\star(s) \\ &- \frac{G_p(s)G_c(s)}{1+G_p(s)G_c(s)} v_d(s) + \frac{1}{1+G_p(s)G_c(s)} G_p(s) i_d(s) \end{aligned} \tag{9}$$

The preceding definitions imply that the loop gain is simply the ratio of the plant to controller impedances. We further denote the voltage and current divider equations as $H_v(s)$ and $H_i(s)$, respectively, to get the following definitions:

$$T(s) := G_p(s)G_c(s) = \frac{z_p(s)}{z_c(s)}, \tag{10}$$

$$H_v(s) := \frac{z_p(s)}{z_p(s)+z_c(s)},\ H_i(s) := \frac{z_c(s)}{z_p(s)+z_c(s)}. \tag{11}$$

The closed-loop response can now be written compactly as

$$v(s) = H_v(s)v^\star(s) - H_v(s)v_d(s) + H_i(s)G_p(s)i_d(s), \tag{12}$$

where it also follows that $H_v(s) = T(s)/(1+T(s))$ and $H_i(s) = 1/(1+T(s))$. We note that in the factors, $T(s)/(1+T(s))$ and $1/(1+T(s))$, are classically known as the *complementary sensitivity* and *sensitivity* functions, respectively, in the controls community [9]. In the controls context, it is well-known that $T(s)/(1+T(s))$ and $1/(1+T(s))$ sum to unity which implies design tradeoffs. In this paper we have established a fundamental link between those quantities and the voltage and current divider equations which also sum to unity (i.e., $H_v(s) + H_i(s) = 1$). The implications of this connection will be revisited later in the paper.

B. Circuit Representations of Prototypical Controllers

Here we consider a generic voltage compensator that can be used in a variety of applications for both constant dc loads and loads with pulsating components. In other words, we seek a compensator model that can be applied to a variety of applications. Consider a proportional-integral-resonant (PIR) controller [11] where the integral and resonant terms give ideal tracking at dc and a resonant frequency ω_r. This gives

$$G_c(s) = \frac{1}{z_c(s)} = k_p + \frac{k_i}{s} + \frac{k_r s}{s^2 + 2\xi\omega_r s + \omega_r^2}. \tag{13}$$

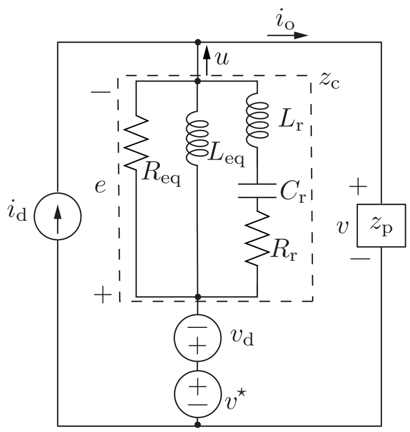

Fig. 4. Equivalent circuit model with a proportional-integral-resonant compensator. The transfer function proportional, integral, and resonant terms translate to resistive, inductive, and RLC tank branches.

To convert (13) to its corresponding circuit representation recall that $G_{\mathrm{c}}(s) = z_{\mathrm{c}}^{-1}(s)$ and equate (13) to

$$z_{\mathrm{c}}^{-1}(s) = R_{\mathrm{eq}}^{-1} + (sL_{\mathrm{eq}})^{-1} + \left(sL_{\mathrm{r}} + R_{\mathrm{r}} + \frac{1}{sC_{\mathrm{r}}}\right)^{-1}. \quad (14)$$

Since $u(s) = z_{\mathrm{c}}^{-1}(s)(v^{\star}(s) - v(s) - v_{\mathrm{d}}(s))$ is a current, it follows that each term in (14) corresponds to a parallel circuit branch where the branch currents sum up to $u(s)$. After some manipulations to (14) and a comparison to (13), we obtain

$$R_{\mathrm{eq}} = \frac{1}{k_{\mathrm{p}}},\ L_{\mathrm{eq}} = \frac{1}{k_{\mathrm{i}}},\ L_{\mathrm{r}} = \frac{1}{k_{\mathrm{r}}},\ C_{\mathrm{r}} = \frac{k_{\mathrm{r}}}{\omega_{\mathrm{r}}^2},\ R_{\mathrm{r}} = \frac{2\xi\omega_{\mathrm{r}}}{k_{\mathrm{r}}}. \quad (15)$$

These relations allow us to straightforwardly translate the parameters of a transfer function $G_{\mathrm{c}}(s)$ to corresponding circuit elements. Ultimately, we arrive at the circuit representation in Fig. 4. Note that PI and PR controllers are easily recovered by eliminating extraneous branches (terms) from the circuit equivalent (transfer function).

C. Closed-loop Circuit Performance

Now consider how classical notions of closed-loop performance translate to the equivalent circuit properties. Traditionally, it is well understood that ideal reference tracking is obtained for frequencies where $\|T(j\omega)\| = \|G_{\mathrm{p}}(j\omega)G_{\mathrm{c}}(j\omega)\| \to \infty$, the compensator $G_{\mathrm{c}}(j\omega)$ has high gain, and hence $\|H_{\mathrm{v}}(j\omega)\| \approx 1$ [12]. From a circuits perspective, recall that $\|T(j\omega)\| = \|z_{\mathrm{p}}(j\omega)/z_{\mathrm{c}}(j\omega)\|$ and the voltage divider is equal to $\|H_{\mathrm{v}}(j\omega)\| = \|z_{\mathrm{p}}(j\omega)/(z_{\mathrm{p}}(j\omega) + z_{\mathrm{c}}(j\omega))\|$. Accordingly, high control gain is equivalent to $\|z_{\mathrm{c}}(j\omega)\| \to 0$, the voltage divider gain approaches unity, and the compensator behaves as a short circuit. Along these lines, ideal tracking at dc and at the resonant frequency, ω_{r}, are obtained with the inductive branch and resonant branches in Fig. 4 which map to integral and resonant terms in $G_{\mathrm{c}}(s)$.
sum to unity, it follows that frequencies with ideal tracking

Shifting our focus to disturbance rejection, recall that the sensitivity function and current divider expression are equivalent such that $\|H_{\mathrm{i}}(j\omega)\| = \|z_{\mathrm{c}}(j\omega)/(z_{\mathrm{p}}(j\omega) + z_{\mathrm{c}}(j\omega))\|$. Furthermore, since the voltage and current divider equations (low value of $\|z_{\mathrm{c}}(j\omega)\|$) also give rejection of the disturbances contained in $i_{\mathrm{d}}(j\omega)$. Expanding on the circuit intuition, this is consistent with $z_{\mathrm{c}}(s)$ shunting $i_{\mathrm{d}}(s)$ away from the load. Lastly since $H_{\mathrm{i}}(j\omega) = 1 - H_{\mathrm{v}}(j\omega)$, it follows that the controller frequency response (and its circuit equivalent) should be tuned to balance reference tracking as well as rejection of voltage sensor noise in $v_{\mathrm{d}}(j\omega)$. Towards that end, the classical strategy of letting $\|T(j\omega)\|$ roll off at high frequencies where noise dominates is tantamount to rising compensator impedance at high frequencies (i.e., $\lim_{\omega\to\infty} \|z_{\mathrm{c}}(j\omega)\| \to \infty$). This is reflected in the inductive branches of $z_{\mathrm{c}}(s)$.

V. Conclusion

We introduced a framework to model voltage controlled DABs as circuit equivalents. Compared to prior art, the proposed model is unique since both the averaged converter and control loop are represented as a unified circuit. Since the controller feedback and feedforward action are represented with an equivalent circuit structure, we reveal a deeper physical intuition of how the closed-loop system operates. Furthermore, we show how the equivalent circuit properties directly map to classical concepts in control analysis. Grounds for future work include the following objectives: i) generalization of circuit equivalent models to other topologies, and ii) application of circuit-based insights to control design.

References

[1] M. N. Kheraluwala, R. W. Gascoigne, D. M. Divan, and E. D. Baumann, “Performance characterization of a high-power dual active bridge dc-to-dc converter,” *IEEE Transactions on Industry Applications*, vol. 28, pp. 1294–1301, Nov 1992.

[2] L. Xue, Z. Shen, D. Boroyevich, P. Mattavelli, and D. Diaz, “Dual active bridge-based battery charger for plug-in hybrid electric vehicle with charging current containing low frequency ripple,” *IEEE Transactions on Power Electronics*, vol. 30, pp. 7299–7307, Dec. 2015.

[3] Y. Shi, R. Li, Y. Xue, and H. Li, “Optimized operation of current-fed dual active bridge DC-DC converter for PV applications,” *IEEE Transactions on Industrial Electronics*, vol. 62, pp. 6986–6995, Nov. 2015.

[4] X. She, A. Q. Huang, and R. Burgos, “Review of solid-state transformer technologies and their application in power distribution systems,” *IEEE Journal of Emerging and Selected Topics in Power Electronics*, Sep. 2013.

[5] M. Cespedes and J. Sun, “Impedance modeling and analysis of grid-connected voltage-source converters,” *IEEE Transactions on Power Electronics*, vol. 29, pp. 1254–1261, March 2014.

[6] X. Wang, L. Harnefors, and F. Blaabjerg, “Unified impedance model of grid-connected voltage-source converters,” *IEEE Transactions on Power Electronics*, vol. 33, pp. 1775–1787, Feb. 2018.

[7] J. Sun, “Small-signal methods for AC distributed power systems - A review,” *IEEE Transactions on Power Electronics*, vol. 24, pp. 2545–2554, Nov. 2009.

[8] J. Sun, “Impedance-based stability criterion for grid-connected inverters,” *IEEE Transactions on Power Electronics*, vol. 26, pp. 3075–3078, Nov. 2011.

[9] S. Skogestad and I. Postlethwaite, *Multivariable Feedback Control*. John Wiley and Sons, 2010.

[10] R. Erickson and D. Maksimovic, *Fundamentals of Power Electronics*. Springer, 2001.

[11] H. Qin and J. W. Kimball, “Closed-loop control of DC-DC dual-active-bridge converters driving single-phase inverters,” *IEEE Transactions on Power Electronics*, Feb. 2014.

[12] R. D. Middlebrook, “The general feedback theorem: a final solution for feedback systems,” *IEEE Microwave Magazine*, vol. 7, pp. 50–63, April 2006.